European Journal of Medicinal Chemistry 65 (2013) 41–50

Contents lists available at SciVerse ScienceDirect

European Journal of Medicinal Chemistry

journal homepage: http://www.elsevier.com/locate/ejmech

Original article

Evaluation of adenine as scaffold for the development of novel P2X3 receptor antagonists

Catia Lambertucci [a,1], Mayya Sundukova [b,1], Dhuldeo D. Kachare [a], Deepak S. Panmand [a], Diego Dal Ben [a], Michela Buccioni [a], Gabriella Marucci [a], Anna Marchenkova [b], Ajiroghene Thomas [a], Andrea Nistri [b], Gloria Cristalli [a], Rosaria Volpini [a,*]

[a] School of Pharmacy, Medicinal Chemistry Unit, University of Camerino, Via S. Agostino, 1, 62032 Camerino, MC, Italy
[b] Neuroscience Department, International School for Advanced Studies (SISSA), Via Bonomea, 265, 34136 Trieste, Italy

ARTICLE INFO

Article history:
Received 14 December 2012
Received in revised form
15 April 2013
Accepted 16 April 2013
Available online 24 April 2013

Keywords:
Purinergic receptors
P2X3 receptor
P2X3 receptor antagonists
Adenine derivatives
Purine derivatives
ATP
Purine
Patch clamp

ABSTRACT

Ligands that selectively block P2X3 receptors localized on nociceptive sensory fibres may be useful for the treatment of chronic pain conditions including neuropathic pain, migraine, and inflammatory pain. With the aim at exploring the suitability of adenine moiety as a scaffold for the development of antagonists of this receptor, a series of 9-benzyl-2-aminoadenine derivatives were designed and synthesized. These new compounds were functionally evaluated at rat or human P2X3 receptors expressed in human embryonic kidney (HEK) cells and on native P2X3 receptors from mouse trigeminal ganglion sensory neurons using patch clamp recording under voltage clamp configuration. The new molecules behaved as P2X3 antagonists, as they rapidly and reversibly inhibited (IC_{50} in the low micromolar range) the membrane currents induced via P2X3 receptor activation by the full agonist α,β-methyleneATP. Introduction of a small lipophilic methyl substituent at the 6-amino group enhanced the activity, in comparison to the corresponding unsubstituted derivative, resulting in the 9-(5-iodo-2-isopropyl-4-methoxybenzyl)-N^6-methyl-9*H*-purine-2,6-diamine (**24**), which appears to be a good antagonist on recombinant and native P2X3 receptors with $IC_{50} = 1.74 \pm 0.21$ μM.

1. Introduction

P2X3 receptors belong to the purinergic P2X receptor class of ligand-gated channels activated by extracellular ATP to induce a rapid increase in membrane permeability to mono- and di-valent cations [1–3]. P2X3 receptors were cloned in 1995 [4,5] and shown to be almost exclusively localized on nociceptive sensory neurons and on afferent fibre terminals in lamina two of the spinal cord dorsal horn [6]. They contribute to pain sensation, visceral mechanosensory transduction, and gut peristalsis [7–10]. Extensive activation of such receptors is believed to be involved in a number of chronic pain conditions including neuropathic pain, which is typically resistant to standard pain treatment, migraine, and inflammatory pain [11]. Functional P2X3 receptors are predominantly expressed as homomers (with fastly desensitizing property upon prolonged exposure to ATP), and to a much lesser extent as heteromers with P2X2 (P2X2/3) [4,5,12]. However, the latter can be distinguished by their insensitivity to low concentrations of the reference non-hydrolysable and selective P2X3 agonist α,β-methyleneATP (α,β-meATP) [12–14]. Targeting these receptors with selective, potent antagonists can represent an innovative approach to treat chronic pain conditions of both neuropathic and inflammatory origin when P2X3 receptor function is reported to be enhanced [15,16]. In the last few years considerable effort has been dedicated to the development of potent and selective antagonists at P2X3 receptors; the first identified P2X3 antagonists were negatively charged and/or high molecular weight organic molecules like suramin, pyridoxalphosphate-6-azophenyl-2′,4′-disulfonic acid (PPADS), 2′,3′-*O*-(2,4,6-trinitrophenyl)-ATP (TNP-ATP) [17], and A-317491 (Fig. 1) [18]; on the other hand, some

Abbreviations: α,β-meATP, α,β-methyleneATP; PPADS, pyridoxalphosphate-6-azophenyl-2′,4′-disulfonic acid; TNP-ATP, 2′,3′-*O*-(2,4,6-trinitrophenyl)-ATP; PPP, triphosphate; HTS, high-throughput screening; TG, trigeminal ganglia; DCM, dichloromethane; NOE, nuclear Overhauser effect; TFAA, trifluoroacetic anhydride; TBAN, tetrabutylammonium nitrate; TEA, triethylamine; PTSA, *p*-toluenesulfonic acid; n_H, Hill coefficient; DRG, dorsal root ganglion; τ_{on}, rise time; $\tau_{des1;2}$, time constant of desensitization decay; CPU, central processing unit; MOE, Molecular Operating Environment; TLC, thin-layer chromatography; PTLC, preparative thin-layer chromatography.

* Corresponding author. Tel.: +39 0737 402278; fax: +39 0737 402295.
E-mail address: rosaria.volpini@unicam.it (R. Volpini).

[1] These authors contributed equally to this work.

0223-5234/$ – see front matter © 2013 Elsevier Masson SAS. All rights reserved.
http://dx.doi.org/10.1016/j.ejmech.2013.04.037

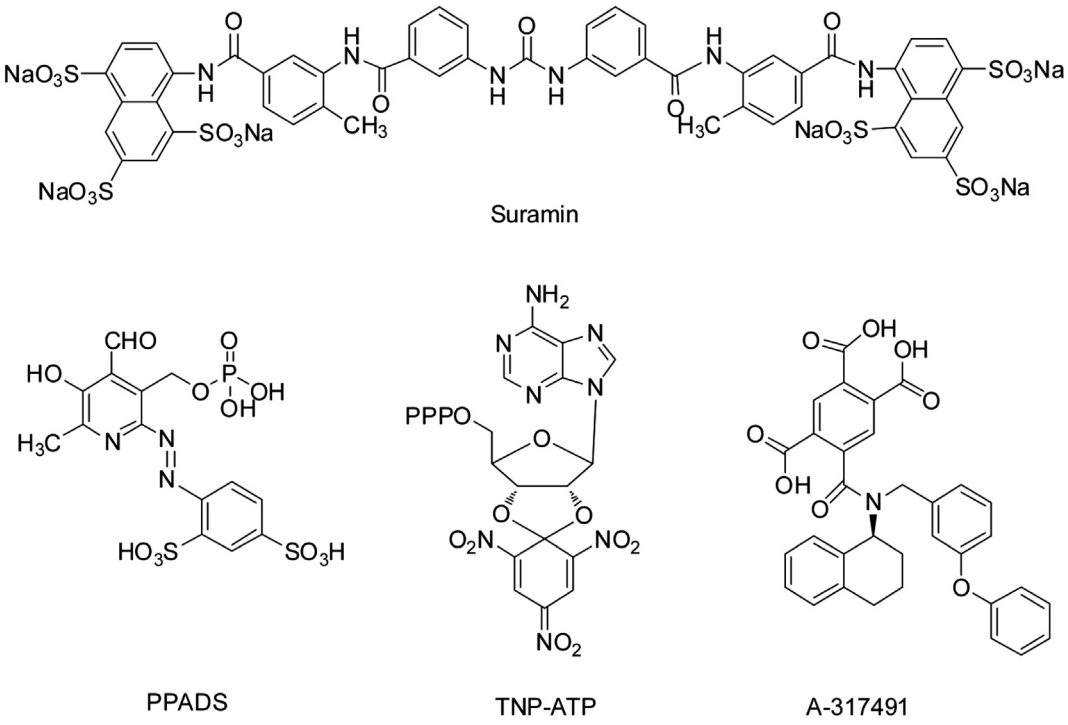

Fig. 1. Structure of some known P2X3 antagonists (PPP = triphosphate).

of them lacked selectivity and potency. The poor pharmacokinetic properties of these molecules (poor oral bioavailability, high protein binding, and uneven tissue distribution) would likely make them unattractive for their development as drugs. More recently, novel antagonists for homomeric P2X3 and heteromeric P2X2/3 receptors, structurally related to the diaminopyrimidine antibacterial drug trimethoprim, have been identified by a high-throughput screening (HTS) campaign [19]. Among them, a compound named RO-3 (Fig. 2A) represents an important step towards discovery of novel drug-like P2X antagonists [20,21] endowed with high affinity and selectivity. Furthermore, new acyclic-nucleotides based on the adenine skeleton and bearing in 9-position a phosphorylated four carbon chain (Fig. 2B) mimicking the ribose function have been described as partial agonists of P2X3 receptors [22].

In the present study, the information coming from the latter two series of above cited compounds was combined with the aim at testing the suitability of the adenine moiety as scaffold for the development of P2X3 antagonists. In detail, a new class of P2X3

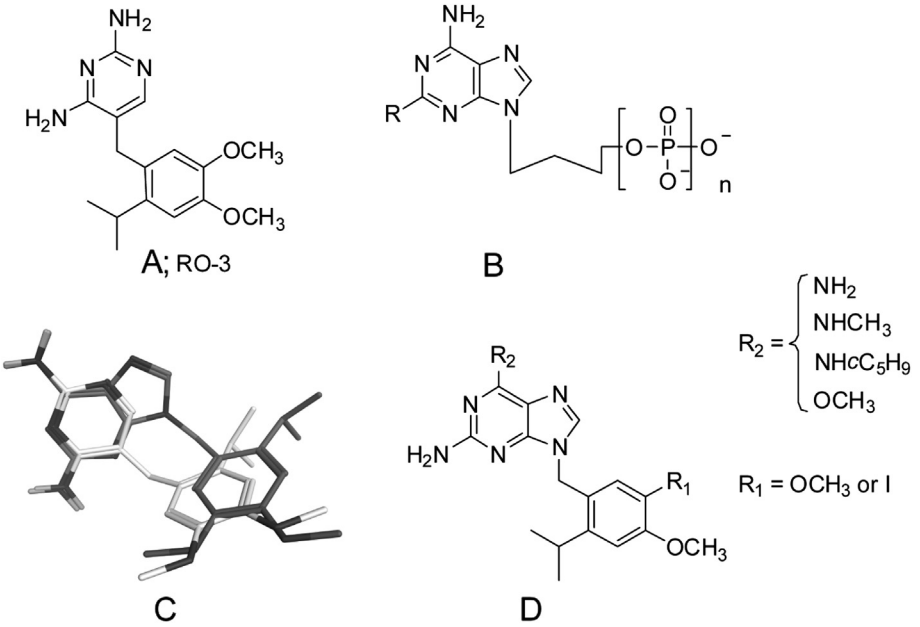

Fig. 2. A and B: known P2X3 ligands; C: 3D alignment of one of the designed purine derivatives (dark grey) with the pyrimidine analogue RO-3 (light grey). Non-polar hydrogen atoms are hidden; D: designed molecules.

ligands was firstly designed by taking into account the structural features of the above mentioned P2X3 receptor antagonists and the adenine scaffold of the partial agonists and by combining this data with the use of molecular modelling tools. A molecular superimposition (Fig. 2C) of the diaminopyrimidine derivative A and the adenine scaffold led to the identification of the 9- and the 2-positions of adenine as possible sites to introduce the substituted aromatic chains and the second amino group observed in diaminopyrimidine series, respectively. As a consequence, 2,6-diaminopurine bearing 2-isopropyl-4,5-dimethoxybenzyl or 5-iodo-2-isopropyl-4-methoxybenzyl chain in 9-position were design ed, synthesized, and tested functionally on P2X3 receptors (Fig. 2D). In order to study the influence of N^6-substitution on P2X3 receptors activity, a methyl and a more sterically hindered cyclopentyl moiety were introduced at N^6-position of these new molecules. Furthermore, the 6-methylamino group was replaced with the isosteric methoxy substituent (Fig. 2D). The new compounds were evaluated for their biological activity on rat and human P2X3 receptors, expressed on human embryonic kidney (HEK) cells and on native P2X3 receptors from mouse trigeminal ganglion (TG) sensory neurons by the patch clamp technique.

2. Results and discussion

2.1. Chemistry

The 9-substituted purine derivatives **21**–**25**, **28** were prepared by alkylating the commercially available 2-amino-6-chloropurine (**16**) with the suitable electrophiles **6** and **15** (Schemes 1–3). For the synthesis of the electrophiles, some intermediates, already reported in literature, were here prepared with different synthetic routes. Experimental details for their synthesis are reported in the Supporting information.

The 2-isopropyl-4,5-dimethoxybenzyl methanesulfonate (**6**) was synthesized starting from the commercially available 3,4-dimethoxy acetophenone (**1**), which was reacted with methyl lithium to give the hydroxy derivative 2-(3,4-dimethoxyphenyl) propan-2-ol (**2**) (Scheme 1). Intermediate alcohol **2** was reduced in the presence of acetic acid, ammonium formate, and a catalytic amount of 10% Pd/C to obtain the corresponding 4-isopropyl-1,2-dimethoxybenzene (**3**).

Formylation of **3** with dichloro(methoxy)methane and tin tetrachloride in dichloromethane (DCM) gave **4**: the synthesis of this compound was also reported in a patent but consisted in a longer route [20]. Compound **4** was then reduced with $NaBH_4$ to (2-isopropyl-4,5-dimethoxyphenyl)methanol (**5**). Mesylation of **5** using methanesulfonyl chloride in the presence of triethylamine gave the desired electrophile **6** (Scheme 1).

The 5-iodo-2-isopropyl-4-methoxybenzyl methanesulfonate (**15**) was synthesized starting from the commercially available 3-methoxyacetophenone (**7**) (Scheme 2). Hence, **7** was reacted with methyl lithium to give the hydroxy derivative 2-(3-methox yphenyl)propan-2-ol (**8**), which was dehydroxylated in the presence of acetic acid, ammonium formate, and catalytic amount of 10% Pd/C, to obtain the corresponding 1-isopropyl-3-methoxy benzene (**9**) [23]. Hence, nitration of compound **9** was performed by reaction with tetrabutylammonium nitrate (TBAN) and trifluoroacetic anhydride (TFAA), in DCM, to obtain the 4-isopropyl-2-methoxy-1-nitrobenzene (**10**). The nitro group of **10** was reduced by hydrogen and 10% Pd/C to furnish the 4-isopropyl-2-methoxyaniline (**11**). 1-Iodo-4-isopropyl-2-methoxybenzene (**12**) was synthesized from **11** by Sandmeyer reaction conditions using *p*-toluenesulfonic acid (PTSA), sodium nitrite, and potassium iodide. Formylation of **12** was achieved by dichloro(methoxy) methane and tin tetrachloride in DCM to furnish **13** (Scheme 2).

The formyl group of **13** was reduced by $NaBH_4$ to give **14**, which was mesylated using the same conditions described for compound **5**, to furnish the desired electrophile **15** (Scheme 2).

After workup, the crude mixtures of mesylates **6** and **15** were reacted with commercially available anhydrous 2-amino-6-chloropurine (**16**) in the presence of K_2CO_3 and 18-crown-6 ether in DMF at 70 °C, to give the desired N9-isomers **17** and **18**, which were obtained as major products along with the N7-regioisomers **19** and **20**, respectively (Scheme 3). The chemical structures of the N9 and N7 isomers were first attributed to compounds **17**, **18** and **19**, **20**, respectively, on the basis of their chemical/physical properties. Firstly, N9-isomers **17** and **18** were obtained in higher yield than the corresponding N7-isomers as it is reported in similar reactions [24]. Secondly, the ^{1}H NMR spectra of the N9-isomers **17** and **18** showed CH_2–N and H-8 signals at higher magnetic field with respect to the corresponding signals of the N7-isomers, **19** and **20**, as reported in literature for analogous compounds (Fig. 3) [24,25].

The N9-isomers, 6-chloro-9-(2-isopropyl-4,5-dimethoxybenzyl)-9*H*-purin-2-amine (**17**) and 6-chloro-9-(5-iodo-2-isopropyl-4-meth oxybenzyl)-9*H*-purin-2-amine (**18**) were reacted with ammonia to

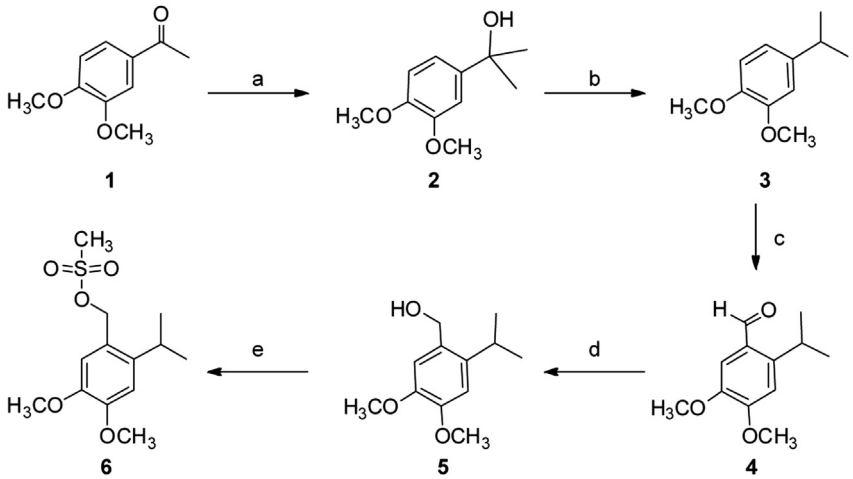

Scheme 1. Reagents and conditions: a. CH_3Li, THF, 69% yield; b. $HCOONH_4$, 10% Pd/C, AcOH, 94% yield; c. Cl_2CHOCH_3, $SnCl_4$, DCM, 92% yield; d. $NaBH_4$, MeOH, 87% yield; e. $MeSO_2Cl$, TEA, DCM, 89% yield.

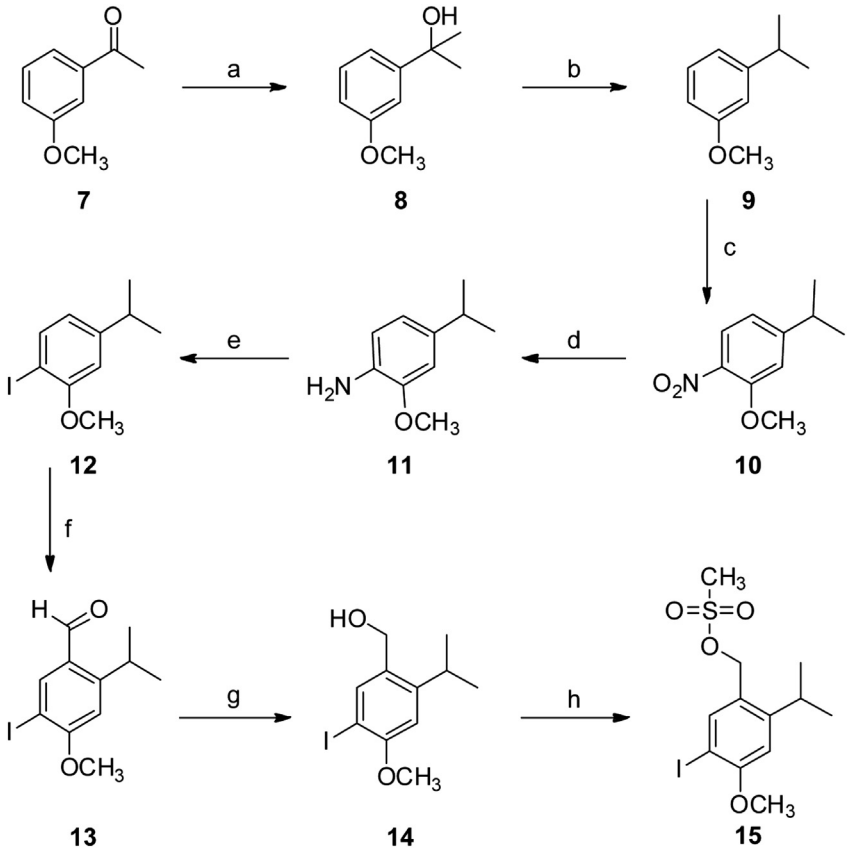

Scheme 2. Reagents and conditions: a. CH_3Li, THF, 77% yield; b. $HCOONH_4$, 10% Pd/C, AcOH, 77% yield; c. TBAN, TFAA, DCM, 77% yield; d. H_2, 10% Pd/C, MeOH, 83% yield; e. PTSA, $NaNO_2$, KI, H_2O/CH_3CN, 65% yield; f. Cl_2CHOCH_3, $SnCl_4$, DCM, 95% yield; g. $NaBH_4$, MeOH, 64% yield; h. $MeSO_2Cl$, TEA, DCM, 92% yield.

obtain compounds **21** and **22**. From the iodomethoxy derivative **18** were also prepared 6-methoxy, 6-methylamino, and 6-cyclopentylamino analogues **23**–**25** by reacting it with sodium methoxide in MeOH, methylamine, and cyclopentylamine, respectively. The two N7-isomers bearing in the 6 position an amino group, **26** and **27**, were prepared from **19** and **20** using the same reaction conditions described above for the corresponding N9-isomers (Scheme 3).

To unequivocally attribute the structure of the N7 and N9-isomers, NOE experiments were performed on 6-amino

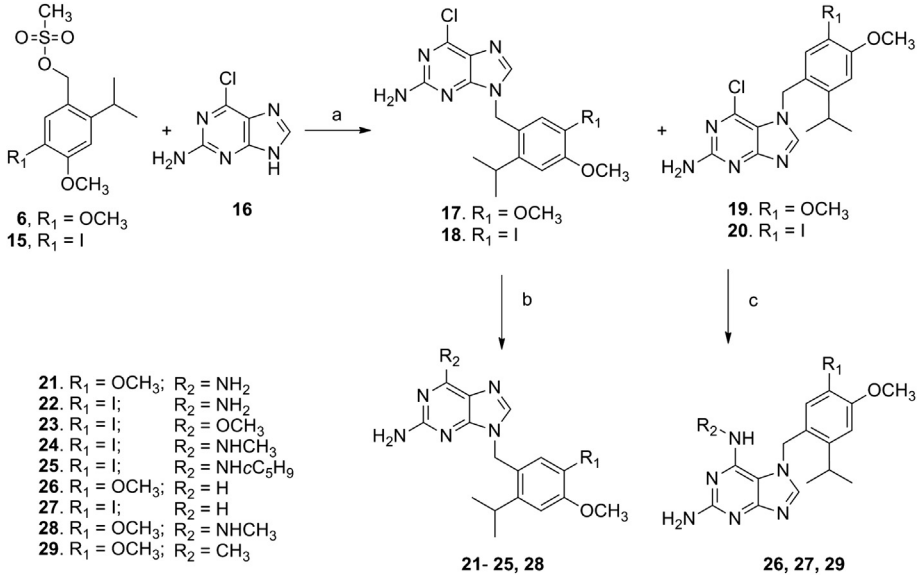

Scheme 3. Reagents and conditions: a. K_2CO_3, 18-crown-6, DMF, yields: **17**–**19** and **20** 51%, 52%, 35%, and 12%, respectively; b. NH_3 liq., or MeONa/MeOH, or CH_3NH_2, or $cC_5H_9NH_2$/THF, yields: **21**–**25** and **28** 54%, 40%, 69%, 76%, 69%, and 40%, respectively; c. NH_3 liq. or CH_3NH_2, yields: **26**, **27**, and **29** 24%, 40%, and 33%, respectively.

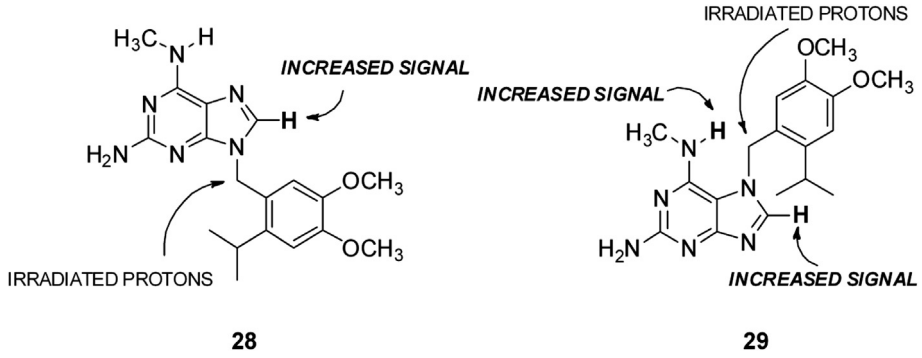

Fig. 3. NOE experiment performed on compound **28** and **29** by irradiation of the signal of CH_2-benzylic group unequivocally permitted to attribute the N9 and N7 isomer structure, respectively.

derivatives **21** and **26** after irradiation of the benzylic CH_2 protons. Results showed increased H-8 signals in ^{1}H NMR spectra of both compounds, but unfortunately no effect was detected at N^6-H_2 hydrogens leaving no possible structure determination. For this reason, the N^6-methylamino derivatives **28** and **29** were prepared from **17** and **19** by reaction with methylamine (Scheme 3). NOE experiments were then performed on **28** and **29** by irradiating the benzylic CH_2 groups. As expected, the intensity of signals for H-8 protons of the two compounds and the N^6-H signal intensity of **29** were increased after irradiation, while no effect was detected on the N^6-H signal of **28**. These data confirmed the structure of the N7-isomer **29**, in which the increased signal intensity of the N^6-H atom was due to the close proximity with the irradiated CH_2 group, which failed to influence the N^6-H signal of **28** owing to its relative distance (Fig. 3).

2.2. Biological assays

2.2.1. Recombinant rat P2X3 receptors expressed in HEK cells

Newly synthesized adenine derivatives **21**–**28**, together with the precursors **17** and **19**, were tested for their biological activity on P2X3 receptors with the patch clamp recording technique. For initial screening, we used rat or human P2X3 receptors transfected into HEK 293T cells, which do not constitutively express them [26,27].

The reference P2X3 agonist α,β-meATP was applied at 100 μM concentration that was reported to elicit maximal effect at this receptor (for full dose–response curve of α,β-meATP at P2X3, see Refs. [26,28,29]; its IC_{50} value is 1.4 μM). All compounds were tested at 100 μM, unless noted, and then the most potent compounds were evaluated also at lower concentrations ranging from 100 to 0.3 μM. Fig. 4 shows the representative trace of the fast desensitizing inward current evoked by α,β-meATP from a HEK 293T cell transfected with rat P2X3 receptors. None of the tested compounds could elicit functional responses even at concentration of 100 μM, except for the rather small and slow current elicited by compound **17** (43 ± 11 pA; 6 ± 2% of control peak of 100 μM α,β-meATP, data not shown). All tested compounds exhibited antagonistic activity on P2X3 receptors, since their continuous application for 20 s blocked subsequent current responses evoked by 2 s pulse of maximal (100 μM) concentration of α,β-meATP with distinct inhibiting potencies. Such inhibition was reversible, as the peak current amplitude fully or partially recovered after 6 min wash out. Inhibition of P2X3-mediated ionic currents induced by compounds **21** and **24** is shown in Fig. 4.

Table 1 shows the calculated percent inhibition of the rat P2X3-mediated currents elicited by tested compounds. At the concentration of 100 μM, the 6-chloro intermediates **17** and **19** showed low inhibition of P2X3 current with a percentage of 27 ± 5% and 19 ± 2%, respectively. The corresponding iodo derivatives **18** and **20** were not tested due to solubility problems. In the series of 6-amino derivatives, the N9-substituted derivatives were more active than the corresponding N7-substituted analogues in all cases. In particular, at 100 μM compound **21** showed 82% inhibition versus compound **26** that showed 23% inhibition, while at 10 μM compound **22** showed higher inhibitory activity versus the corresponding N7 isomer **27** (78% versus 43% inhibition, respectively). Compound **27** was not tested at 100 μM due to solubility problems. Among these compounds the presence of an iodine atom in the benzyl chain instead of a methoxy group favoured the P2X3

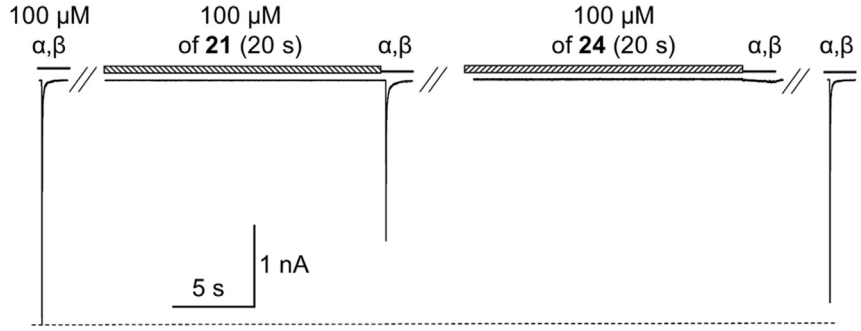

Fig. 4. Effect of **21** and **24** on rat P2X3 receptors expressed by HEK cells. Typical rapidly desensitizing inward current evoked by 100 μM α,β-meATP (α,β in the figure) was taken as control peak current (dashed line). After 20 s application of test compound **21** (100 μM; via fast superperfusion), subsequent application of 100 μM α,β-meATP induced peak current amplitude smaller than the reference one. Application of 100 μM test compound **24** exerted more potent inhibition of P2X3 activity. After 6 min wash out (time necessary for recovery from α,β-meATP-induced desensitization), the current amplitude was almost completely restored.

Table 1
Summary of antagonism activity of novel adenine derivatives.

Compound	Concentration, μM	Inhibition of P2X3 current, %
17	100	27 ± 5
19	100	19 ± 2
21	1	8 ± 4
	10	36 ± 2
	100	82 ± 2
22	0.3	23 ± 7
	1	35 ± 3
	10	78 ± 7
	100	93 ± 2
23	100	50 ± 6
24	0.3	22 ± 4
	1	41 ± 3
	10	76 ± 5
	100	98 ± 1
25	0.3	45 ± 3
	1	51 ± 3
	10	60 ± 10
	100	58 ± 6
26	100	23 ± 7
27	10	43 ± 10
28	100	71 ± 5

Effects of the novel compounds were investigated on P2X3 currents evoked by 100 μM α,β-meATP; inhibition is expressed as % amplitude of control α,β-meATP-evoked current; data are from 5 to 14 experiments.

inhibition activity (see **22**: 78% versus **21**: 82% and **24**: 98% versus **28**: 71%). Replacement in compound **22** of the 6-NH_2 group with the methoxy substituent strongly decreased the activity (compare **22** and **23** at 100 μM: 93% and 50%, respectively). On the other hand, the presence of a small alkyl group at the N^6-position gave a further enhancement of the inhibitory activity (compounds tested at 100 μM), which decreased when a more hindered cyclopentyl was introduced in the same position (at 100 μM **22**: 93% inhibition, **24**: 98% inhibition, and **25**: 58% inhibition). At lower concentration, there was a dose-dependent decrease of the inhibition; although compound **25** produced a relatively strong inhibition (45%) at submicromolar concentration, its antagonism saturated at approximately 60% despite the application of 100 μM. The N^6-methyl derivative **24**, bearing the iodobenzyl chain, resulted in the most potent P2X3 receptors inhibitor of the series with an almost complete inhibition of the full agonist evoked currents and a significant residual 22% inhibition also at the lowest tested concentration of 0.3 μM.

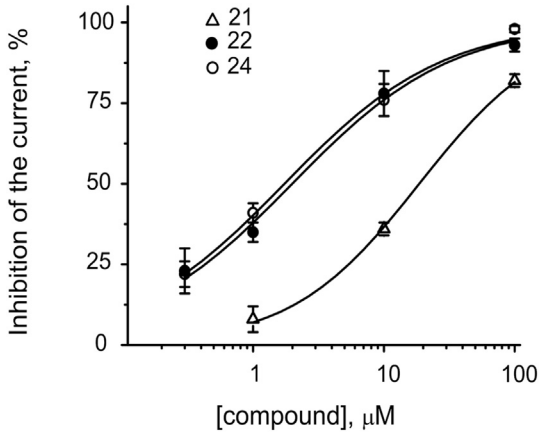

Fig. 5. Dose–inhibition curves of P2X3-mediated currents for compounds **21**, **22**, and **24** built by applying different concentrations of antagonists using the same concentration of agonist (100 μM α,β-meATP). Data points from $n = 6$–14 cells, fitted with Hill equation (Eq. (2)).

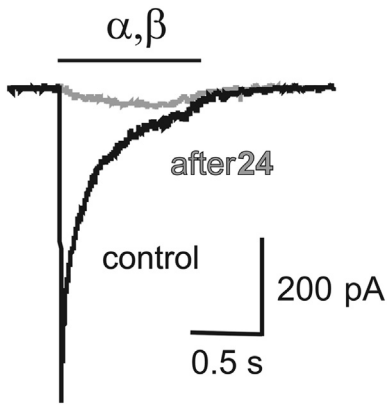

Fig. 6. Representative traces of α,β-meATP evoked P2X3 currents in control (black) and after pre-application of compound **24** (grey) from a TG neuron, superimposed. Note the almost complete suppression of the current after compound application.

Inhibition–response curves were built for the most potent compounds (**21**, **22**, and **24**) as demonstrated in Fig. 5, in which log compound concentration was plotted against the percent depression of the α,β-meATP evoked current. Fitting the data with Hill equation (Eq. (2): see experimental details) yielded for compound **22** a value of $IC_{50} = 2.23 \pm 0.29$ μM with $n_H = 0.6 \pm 0.1$, for compound **24** a value of $IC_{50} = 1.74 \pm 0.21$ μM with $n_H = 0.7 \pm 0.1$, and

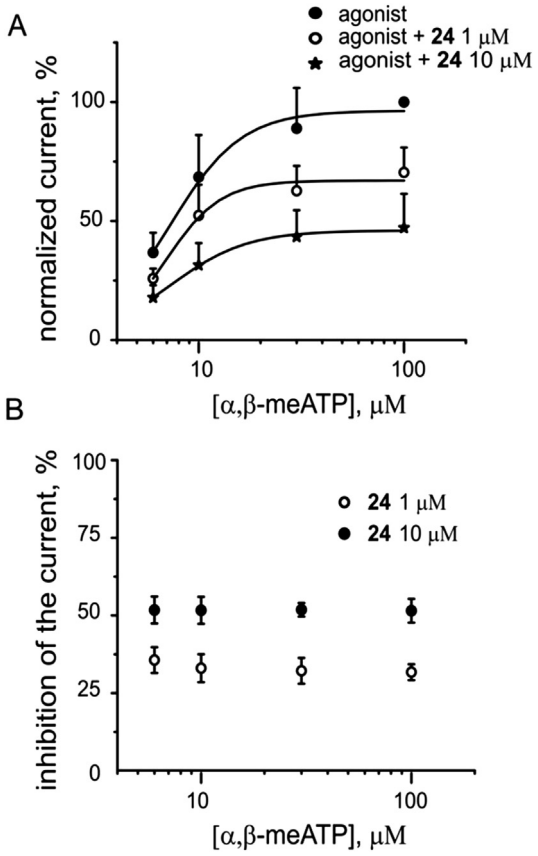

Fig. 7. A. Concentration–response curves for α,β-meATP-evoked rat P2X3 currents in control and with pre-application of increasing concentrations of compound **24** were fitted with empirical Hill equation (Eq. (2) see Experimental section). EC_{50} values for α,β-meATP were 7.2 ± 1.6 μM for control, 6.9 ± 1.0 μM in the presence of 1 μM of **24** and 7.2 ± 2.3 μM in the presence of 10 μM of **24**. B. The data from A re-plotted in terms of inhibition of currents by various concentrations of compound **24** *vs* log concentration of agonist α,β-meATP. Data presented from 5 to 17 cells.

for compound **21** $IC_{50} = 18.6 \pm 0.9$ μM with $n_H = 0.9 \pm 0.1$ ($n = 6$–14 cells, Table 1).

2.2.2. Recombinant human P2X3 receptors

We next enquired if human P2X3 receptors transiently expressed by HEK cells were equi-sensitive to the novel antagonist compound **24** (that was most effective on rat receptors). Human P2X3 currents induced by 100 μM α,β-meATP were almost completely blocked by 20 s pre-application of compound **24** (100 μM). We also tested if compound **24** could block the α,β-meATP current even at the concentrations of 1 μM and 10 μM. Indeed, the percent inhibition of human P2X3 receptor activity was 29 ± 2% (compared with the one of rat P2X3 receptor: 40 ± 3%, $n = 5$), thus, slightly less intense than the blocking action on rodent receptors. Fitting inhibition–response curve with Hill equation yielded for compound **24** a value of $IC_{50} = 2.2 \pm 0.1$ μM with $n_H = 1.1 \pm 0.1$ ($n = 2$–5 cells).

2.2.3. Native receptors in trigeminal ganglion neurons

Since 100 μM of compound **24** produced the strongest inhibition of P2X3 receptors expressed by HEK cells, it was important to test the sensitivity of native P2X3 receptors expressed by TG sensory neurons in culture. Fig. 6 shows an example of α,β-meATP-evoked inward current recorded from a TG neuron and its near-full inhibition by compound **24** (100 μM). At 1 μM the percent inhibition of the current was 37 ± 3% ($n = 7$), hence compound **24** had similar antagonistic potency on recombinant and native P2X3 receptors.

To assess the nature of the mechanism antagonist–receptor interaction, we tested how efficiently compound **24** at different concentrations inhibited the P2X3 currents evoked by different concentrations of the agonist α,β-meATP. As the level of inhibition was similar for the wide range of agonist concentration (low and high concentrations, see Fig. 7), we hypothesize that compound **24** behaves as non-competitive antagonist. However, we cannot exclude that the nature of antagonism is of a mixed type.

3. Conclusions

This study was aimed at testing the adenine moiety as possible new scaffold for the development of P2X3 antagonists. The designed series of 2-aminoadenine derivatives was synthesized and tested on recombinant rat P2X3 receptors expressed in HEK cells, by using patch clamp recording technique. The novel compounds showed to behave as P2X3 receptor antagonists, the N9-isomers being more active than the corresponding N7 analogues. Introduction at the 6-amino group of a small lipophilic substituent increased the potency at least in the series containing the iodo atom within the substituted benzyl chain, resulting in the 9-(5-iodo-2-isopropyl-4-methoxybenzyl)-N^6-methyl-9*H*-purine-2,6-diamine (**24**), which is the most active compound of the presented derivatives (at 100 μM) and appears to be a good antagonist on recombinant and native P2X3 receptors with IC_{50} in the low μM range.

The effect of the introduction of a methyl group in N^6-position was an increase of activity respect to the corresponding unsubstituted compound (at 100 μM; **22**: 93% activity *vs* **24**: 98% activity).

In conclusion, biological results show that the synthesised adenine-based compounds possess antagonist activity at P2X3 receptors, even if with lower potency respect to the corresponding diaminopyrimidines taken as reference compounds. These results are encouraging as the versatility of the adenine scaffold allows the insertion of different substituents in several position of the purine moiety itself. The investigation on the effect of these modifications on P2X3 receptor antagonist activity could help for the development of new agents for the treatment of neuropathic pain, migraine, and inflammatory pain.

4. Experimental section

4.1. Molecular modelling

All molecular modelling studies were performed on a 2 CPU (PIV 2.0–3.0 GHz) Linux PC. Rebuilding of analysed compound structures was carried out using Molecular Operating Environment (MOE, version 2010.10) suite [30]. All ligand structures were optimized using RHF/AM1 semiempirical calculations and the software package MOPAC [31] implemented in MOE was utilized for these calculations. Superimposition of molecules was performed by using the Flexible Alignment tool of MOE.

4.2. Chemistry

Melting points were determined with a Büchi apparatus B-540. ^{1}H NMR spectra were obtained with Varian Mercury 400 MHz spectrometer; δ in ppm, J in Hz. All exchangeable protons were confirmed by addition of D_2O. Thin-layer chromatography (TLC) was carried out on pre-coated TLC plates with silica gel 60 F-254 (Merck) and preparative thin-layer chromatography (PTLC) on pre-coated plates with silica gel 60 Å Analtech. For column chromatography, silica gel 60 (Merck) was used. Mass spectra were recorded on an HP 1100-MSD series instrument. All measurements were performed using electrospray ionization (ESI-MS) on a single quadrupole analyzer. Elemental analyses were determined on a Fisons model EA 1108 CHNS–O model analyser and are within ±0.4% of theoretical values. Purity of the compounds was ≥95% according to elemental analysis data. See the Supporting information for further information.

4.3. General procedure for the preparation of compounds *17–20*

K_2CO_3 (0.452 g, 3.27 mmol) was added to stirred solution of mesyl compound **6** or **15** (2.73 mmol) in dry DMF (12 mL). 2-Amino-6-chloropurine (**16**) (0.506 g, 2.73 mmol) and 18-crown-6 (1 mg) were added after 5 min and reaction was left at 65 °C for 12 h. Then reaction mixture was partitioned between EtOAc and water. The combined organics were washed with saturated solution of $NaHCO_3$ and brine, and then they were dried over Na_2SO_4, concentrated under reduced pressure and the residue was chromatographed over flash silica gel column using the appropriate eluent to obtain compounds **17–20** as white solids.

*4.3.1. 6-Chloro-9-(2-isopropyl-4,5-dimethoxybenzyl)-9H-purin-2-amine (**17**) and 6-chloro-7-(2-isopropyl-4,5-dimethoxybenzyl)-7H-purin-2-amine (**19**)*

Compounds **17** and **19** were obtained from **6** after flash silica gel column chromatography eluting with $CHCl_3$–MeOH (99.75:0.25–97:3, v/v) as white solids. **17**: Yield 51%; mp 161–163 °C. ^{1}H NMR (DMSO-d_6): δ 1.02 (d, 6H, J = 6.8 Hz, CH(CH_3)$_2$), 3.19 (sept, 1H, J = 6.8 Hz, CH(CH_3)$_2$), 3.68 (s, 3H, OCH_3), 3.74 (s, 3H, OCH_3), 5.19 (s, 2H, NCH_2), 6.84 (s, 1H, H–Ph), 6.91 (s, 1H, H–Ph), 6.93 (brs, 2H, NH_2), 7.95 (s, 1H, H-8). **19**: Yield 35%; mp 193–195 °C. ^{1}H NMR (DMSO-d_6): δ 1.12 (d, 6H, J = 6.8 Hz, CH(CH_3)$_2$), 3.13 (sept, 1H, J = 6.8 Hz, CH(CH_3)$_2$), 3.52 (s, 3H, OCH_3), 3.76 (s, 3H, OCH_3), 5.51 (s, 2H, NCH_2), 6.33 (s, 1H, H–Ph), 6.67 (brs, 2H, NH_2), 6.90 (s, 1H, H–Ph), 8.12 (s, 1H, H-8).

4.3.2. 6-Chloro-9-(5-iodo-2-isopropyl-4-methoxybenzyl)-9H-purin-2-amine (**18**) and 6-chloro-7-(5-iodo-2-isopropyl-4-methoxybenzyl)-7H-purin-2-amine (**20**)

Compounds **18** and **20** were obtained from **15** after flash chromatography eluting with CH_2Cl_2–MeCN (98:2, v/v) as white solids. **18**: Yield 52%; mp 120–122 °C. ^{1}H NMR (DMSO-d_6): δ 1.08 (d, 6H, J = 6.8 Hz, CH(CH_3)$_2$), 3.20 (sept, 1H, J = 6.8 Hz, CH(CH_3)$_2$), 3.82 (s, 3H, OCH_3), 5.20 (s, 2H, NCH_2), 6.89 (s, 1H, H–Ph), 6.95 (s, 2H, NH_2), 7.47 (s, 1H, H–Ph), 7.99 (s, 1H, H-8); and CH_2Cl_2–MeCN (96:04, v/v). **20**: Yield 12%; mp 140–142 °C. ^{1}H NMR (DMSO-d_6): δ 1.18 (d, 6H, J = 6.8 Hz, CH(CH_3)$_2$), 3.10 (sept, 1H, J = 6.8 Hz, CH(CH_3)$_2$), 3.83 (s, 3H, OCH_3), 5.52 (s, 2H, NCH_2), 6.71 (brs, 2H, NH_2), 6.88 (s, 1H, H–Ph), 6.94 (s, 1H, H–Ph), 8.27 (s, 1H, H-8).

4.4. General procedure for the preparation of compounds **21** and **22**

Ammonia gas was condensed at −70 °C in cooled steel vial then starting material **17** or **18** was added and reaction mixture was maintained at room temperature for 16 h. Volatiles were removed and crude mixture was partitioned between EtOAC and H_2O. Then combined organics were washed with saturated solution of NH_4Cl, dried over Na_2SO_4 and concentrated under reduced pressure to obtain crude product **21** or **22**, respectively.

4.4.1. 9-(2-Isopropyl-4,5-dimethoxybenzyl)-9H-purine-2,6-diamine (**21**)

Compound **21** was obtained from **17** after crystallization from MeOH, as white solid. Yield 54%; mp 198–200 °C. ^{1}H NMR (DMSO-d_6): δ 1.03 (d, 6H, J = 6.4 Hz, CH(CH_3)$_2$), 3.18 (sept, J = 6.4 Hz, 1H, CH(CH_3)$_2$), 3.66 (s, 3H, OCH_3), 3.74 (s, 3H, OCH_3), 5.08 (s, 2H, NCH_2), 5.78 (brs, 2H, NH_2), 6.64 (brs, 2H, NH_2), 6.84 (s, 1H, H–Ph), 6.89 (s, 1H, H–Ph), 7.46 (s, 1H, H-8); ESI-MS: positive mode m/z 343.1 ($[M + H]^+$), 365.1 ($[M + Na]^+$).

4.4.2. 9-(5-Iodo-2-isopropyl-4-methoxybenzyl)-9H-purine-2,6-di amine (**22**)

Compound **22** was obtained from **18** after flash silica gel column chromatography eluting with $CHCl_3$–MeOH (98:2–95:5, v/v) as white solids. Yield 40%; mp 230–232 °C. ^{1}H NMR (DMSO-d_6): δ 1.14 (d, 6H, J = 6.8 Hz, CH(CH_3)$_2$), 3.09 (sept, 1H, J = 6.8 Hz, CH(CH_3)$_2$), 3.82 (s, 3H, OCH_3), 5.46 (s, 2H, NCH_2), 5.55 (s, 2H, NH_2), 6.29 (s, 2H, NH_2), 6.91 (s, 1H, H–Ph), 7.65 (s, 1H, H-8), 7.08 (s, 1H, H–Ph); ESI-MS: positive mode m/z 439.0 ($[M + H]^+$), 461.0 ($[M + Na]^+$), 477.0 ($[M + K]^+$).

4.4.3. 9-(5-Iodo-2-isopropyl-4-methoxybenzyl)-6-methoxy-9H-purin-2-amine (**23**)

A suspension of **18** (50 mg, 0.10 mmol) and sodium methoxide (53 mg, 0.98 mmol) in dry CH_3OH (2 mL) was refluxed for 2 h. Then solvent was evaporated and the resulted residue was extracted with EtOAc and water. Combined organics were washed with saturated NH_4Cl solution, dried over anhydrous Na_2SO_4, and evaporated to dryness. The crude was crystallized from MeCN to give **23** as white solid. Yield 69%; mp 212–214 °C. ^{1}H NMR (DMSO-d_6): δ 1.08 (d, 6H, J = 6.8 Hz, CH(CH_3)$_2$), 3.21 (sept, 1H, J = 6.8 Hz, CH(CH_3)$_2$), 3.81 (s, 3H, OCH_3), 3.95 (s, 3H, OCH_3), 5.17 (s, 2H, NCH_2), 6.43 (s, 2H, NH_2), 6.89 (s, 1H, H–Ph), 7.37 (s, 1H, H–Ph), 7.71 (s, 1H, H-8); ESI-MS: positive mode m/z 454.0 ($[M + H]^+$), 492.0 ($[M + K]^+$), 929.0 ($[2M + Na]^+$).

4.4.4. 9-(5-Iodo-2-isopropyl-4-methoxybenzyl)-N^6-methyl-9H-purine-2,6-diamine (**24**)

To a suspension of **18** (50 mg, 0.10 mmol) in dry THF (2 mL) was added methylamine (1.5 mL, 33.80 mmol) at −20 °C and reaction mixture was left for 3 h at room temperature, then solvent was evaporated and the resulting residue was extracted with EtOAc. The combined organics were washed with water, dried over anhydrous Na_2SO_4, concentrated and the crude was crystallized from MeCN to give **24** as white solid. Yield 76%; mp 238–240 °C. ^{1}H NMR (DMSO-d_6): δ 1.09 (d, 6H, J = 6.8 Hz, CH(CH_3)$_2$), 2.86 (s, 3H, $NH$$CH_3$), 3.20 (sept, 1H, J = 7.2 Hz, CH(CH_3)$_2$), 3.81 (s, 3H, OCH_3), 5.10 (s, 2H, NCH_2), 5.85 (s, 2H, NH_2), 6.88 (s, 1H, H–Ph), 7.21 (s, 1H, $NH$$CH_3$), 7.37 (s, 1H, H–Ph), 7.50 (s, 1H, H-8); ESI-MS: positive mode m/z 453.0 ($[M + H]^+$), 475.0 ($[M + Na]^+$).

4.4.5. N^6-Cyclopentyl-9-(5-iodo-2-isopropyl-4-methoxybenzyl)-9H-purine-2,6-diamine (**25**)

A suspension of **18** (0.050 g, 0.10 mmol) and cyclopentylamine (1.02 mL, 10.40 mmol) in dry THF (2 mL) was stirred for 30 h at 60 °C. Then solvent was evaporated and the resulted residue was extracted with EtOAc. The combined organics were washed with water, dried over anhydrous Na_2SO_4, evaporated under vacuo and the crude was chromatographed over flash silica gel column eluting with $CHCl_3$–MeCN (98:2, v/v) to give **25** as white solid. Yield 69%; mp 182–184 °C. ^{1}H NMR (DMSO-d_6): δ 1.09 (d, 6H, J = 6.8 Hz, CH(CH_3)$_2$), 1.50 (m, 4H, H-cyclopentyl), 1.68 (m, 2H, H-cyclopentyl), 1.88 (m, 2H, H-cyclopentyl), 3.20 (sept, 1H, J = 6.8 Hz, CH(CH_3)$_2$), 3.81 (s, 3H, OCH_3), 4.44 (m, 1H, NHCH), 5.10 (s, 2H, NCH_2), 5.80 (brs, 2H, NH_2), 6.88 (s, 1H, H–Ph), 7.06 (brs, 1H, NH), 7.38 (s, 1H, H–Ph), 7.51 (s, 1H, H-8); ESI-MS: positive mode m/z 507.1 ($[M + H]^+$), 529.0 ($[M + Na]^+$).

4.5. General procedure for the preparation of compounds (**26** and **27**)

Ammonia gas was condensed at −70 °C in steel vial then starting material **19** or **20** was added and reaction mixture maintained at 100 °C for 16 h in well packed steel vial. Volatiles were removed and the residue was partitioned between EtOAC and H_2O; the combined organics were washed with saturated solution of NH_4Cl, dried over the Na_2SO_4 and concentrated under reduced pressure. The residue was purified by flash column chromatography.

4.5.1. 7-(2-Isopropyl-4,5-dimethoxybenzyl)-7H-purine-2,6-diamine (**26**)

Compound **26** was obtained from **19** after flash silica gel column chromatography eluting with $CHCl_3$–MeOH (98:2–92:8, v/v) as white solid. Yield 24%; mp 245–247 °C. ^{1}H NMR (DMSO-d_6): δ 1.09 (d, 6H, J = 6.8 Hz, CH(CH_3)$_2$), 3.03 (sept, 1H, J = 6.8 Hz, CH(CH_3)$_2$), 3.57 (s, 3H, OCH_3), 3.75 (s, 3H, OCH_3), 5.42 (s, 1H, NCH_2), 5.51 (brs, 2H, NH_2), 6.32 (brs, 2H, NH_2), 6.57 (s, 1H, H–Ph), 6.89 (s, 1H, H–Ph), 7.51 (s, 1H, H-8); ESI-MS: positive mode m/z 343.1 ($[M + H]^+$), 685.3 ($[2M + H]^+$), 707.3 ($[2M + Na]^+$).

4.5.2. 7-(5-Iodo-2-isopropyl-4-methoxybenzyl)-7H-purine-2,6-diamine (**27**)

Compound **27** was obtained from **20** after flash silica gel column chromatography eluting with $CHCl_3$–MeOH (98:2–95:5, v/v) as white solid. Yield 40%; mp 240–242 °C. ^{1}H NMR (DMSO-d_6): δ 1.14 (d, 6H, J = 6.8 Hz, CH(CH_3)$_2$), 3.09 (sept, 1H, J = 6.8 Hz, CH(CH_3)$_2$), 3.82 (s, 3H, OCH_3), 5.46 (s, 2H, NCH_2), 5.55 (s, 2H, NH_2), 6.29 (s, 2H, NH_2), 6.91 (s, 1H, H–Ph), 7.08 (s, 1H, H–Ph), 7.65 (s, 1H, H-8); ESI-MS: positive mode m/z 439.0 ($[M + H]^+$), 877.2 ($[2M + H]^+$), 899.0 ($[2M + Na]^+$), 915.0 ($[2M + K]^+$).

4.6. General procedure for the preparation of compounds (**28** and **29**)

To compound **17** or **19** (0.22 mmol), taken in steel vessel at −70 °C, methylamine (1.0 mL) was added. The reaction was left for 1 day at room temperature, volatiles were then removed and the crude mixture was purified by silica gel flash column chromatography eluting with the suitable solvent.

4.6.1. 9-(2-Isopropyl-4,5-dimethoxybenzyl)-N^6-methyl-9H-purine-2,6-diamine (**28**)

Compound **28** was obtained from **17** after flash silica gel column chromatography eluting with CH_2Cl_2–CH_3OH (97:3, v/v) as white solid. Yield 40%; mp 188–190 °C. ^{1}H NMR (DMSO-d_6): δ 1.02 (d, 6H, J = 7.2 Hz, CH(CH_3)$_2$); 2.85 (br m, 3H, NHCH_3), 3.18 (m, 1H, CH(CH$_3$)$_2$), 3.65 (s, 3H, OCH$_3$); 3.73 (s, 3H, OCH$_3$); 5.08 (s, 2H, CH$_2$); 5.84 (brs, 2H, NH$_2$); 6.83 (s, 1H, H–Ph); 6.88 (s, 1H, H–Ph); 7.15 (brs, 1H, NH); 7.44 (s, 1H, H-8); ESI-MS: positive mode m/z 357.4 ([M + H]$^+$), 379.5 ([M + Na]$^+$), 735.8 ([2M + Na]$^+$).

4.6.2. 7-(2-Isopropyl-4,5-dimethoxybenzyl)-N^6-methyl-7H-purine-2,6-diamine (**29**)

Compound **29** was obtained from **19** after silica gel flash column chromatography eluting with CH_2Cl_2–CH_3OH (95:5, v/v) as white solid. Yield 33%; mp 254–256 °C. ^{1}H NMR (DMSO-d_6): δ 1.09 (d, 6H, J = 6.8 Hz, CH(CH_3)$_2$); 2.86 (d, 3H, J = 4.4 Hz, NHCH_3), 3.01 (sept, 1H, J = 6.8 Hz, CH(CH$_3$)$_2$), 3.59 (s, 3H, OCH$_3$), 3.76 (s, 3H, OCH$_3$), 5.42 (s, 2H, CH$_2$), 5.63 (brs, 2H, NH$_2$), 6.46 (bs, 1H, NHCH$_3$), 6.65 (s, 1H, H–Ph), 6.89 (s, 1H, H–Ph), 7.38 (s, 1H, H-8); ESI-MS: positive mode m/z 357.2 ([M + H]$^+$), 713.5 ([2M + H]$^+$), 735.5 ([2M + Na]$^+$).

4.7. Biological assay

4.7.1. Recombinant P2X3 receptors

Experiments were performed in accordance with our recent reports [22,32]. In brief, HEK 293T cells, supplied by the in-house SISSA bank, were cultured in Dulbecco's Modified Eagle Medium (DMEM) supplemented with 10% foetal bovine serum (FBS), Glutamax and antibiotics in an incubator (5% CO_2/95% humidity, 37 °C). Cells were placed on poly-L-lysine coated 35 mm Petri dishes and transiently transfected by the calcium phosphate technique with pEGFP (Clontech, Mountain View, CA) and pcDNA3-P2X3 plasmids (0.5 μg/mL each; 1:1 ratio). Rat and human pcDNA3-P2X3 constructs (NCBI accession numbers CAA62594 and AAH74793, respectively) were kindly provided by Prof. R.A. North (University of Manchester, UK). Twenty four or 48 h later transfected cells were used for experiments, because P2X3 expression was found to be comparable at these time points, probed by immunofluorescence and western blotting.

4.7.2. Trigeminal ganglia culture neurons

Cultures of trigeminal ganglion sensory neurons were prepared from C57Bl/6 wild type mice (P10–14) as previously described [33]. In brief, trigeminal ganglia were rapidly excised and enzymatically dissociated in F12 medium (Invitrogen Corp, Milan, Italy) containing 0.25 mg/mL trypsin, 1 mg/mL collagenase, 0.2 mL DNAse (Sigma, Milan, Italy) at 37 °C for 12 min. Cells were plated on poly-L-lysine coated 35 mm Petri dishes on F12 medium supplemented with 10% foetal bovine serum and antibiotics and incubated for 24 h (5% CO_2/95% humidity, 37 °C).

4.7.3. Patch clamp recordings

Currents were recorded from small/medium size mouse TG neurons (nociceptors that strongly express native P2X3 receptors [33]) or single GFP-positive (visualized by fluorescent microscopy) HEK cells as previously described [32,33] under whole cell voltage clamp mode at a holding potential of −60 mV. Cells were continuously superfused at room temperature with control solution containing (in mM): 152 NaCl, 5 KCl, 1 $MgCl_2$, 2 $CaCl_2$, 10 glucose, 10 HEPES; pH 7.4 adjusted with NaOH. Patch pipettes had a resistance of 3–4 MΩ when filled with (in mM): 140 KCl, 2 $MgCl_2$, 0.5 $CaCl_2$, 2 ATP–Mg, 2 GTP–Li, 20 HEPES, 5 EGTA; pH 7.2 adjusted with KOH (for recordings from TG neurons) and 130 CsCl, 20 HEPES, 1 $MgCl_2$, 3 ATP–Mg, EGTA 5, pH 7.2 adjusted with CsOH (for HEK cells). Data were acquired and analysed with the pCLAMP software Clampex 9.2 (Molecular Devices, Palo Alto, CA, USA). After obtaining whole cell configuration, cell slow capacitance was compensated. Access resistance was never >10 MΩ and was routinely compensated by at least 70%.

4.7.4. Drug application and data analysis

The receptor agonists α,β-meATP (Sigma) and test compounds were applied by rapid solution changer system (Perfusion Fast-Step System SF-77B, Warner Instruments, Hamden, CT, USA). Unless otherwise stated, α,β-meATP was applied at 100 μM concentration that is known to produce a maximal inward current response [26,28,29]. Membrane currents were analysed in terms of their peak amplitude and rise time (10–90% of the peak). Current decay due to receptor desensitization during agonist application was fitted with either a monoexponential or biexponential function using pCLAMP Clampfit 9.2.

Test compounds were kept at +4 °C and dissolved to 10 mM in DMSO or DMSO–H_2O (1:1) or DMSO–HCl (18% 1 N) before experiments and then diluted to necessary concentration in control solution. For routine tests, α,β-meATP was applied at 100 μM concentration (2 s pulse) at least 3 times (at 5 min interval to prevent cumulative receptor desensitization) to obtain an average control response. Since activated P2X3 receptors desensitize rapidly in the sustained presence of agonist, the inward current transient is, of course, too short for the binding equilibrium to be reached when agonist and antagonist are co-applied. Thus, to assess potential receptor blocking activity, each test compound was continuously pre-applied for 20 s before the α,β-meATP application as done previously [22,28]. Antagonist activity was quantified as percent inhibition of the α,β-meATP-induced current:

$$\%\,\text{inhibition} = 100 \times (1 - I_2/I_1), \quad (1)$$

where I_1 is the control peak current, I_2 is the peak amplitude of the current after test compound.

For the most potent compounds, antagonist dose–inhibition curves were constructed by applying for 20 s different concentrations of each test compound using the same maximal concentration (100 μM) of α,β-meATP agonist. Data were plotted and fitted with empirical Hill equation using Origin 6.0 (Microcal, Northampton, MA, USA):

$$\%\,\text{inhibition} = 100/(1 + (IC_{50}/[\text{Ant}])^{n_H}), \quad (2)$$

where [Ant] is the concentration of the antagonist, n_H is the Hill coefficient, IC_{50} is the concentration of antagonist required to block the maximal current by 50%. Agonist concentration–response curves in terms of normalized currents *vs* log agonist concentration were fitted with the same Hill equation, with corresponding parameters EC_{50} and n_H, where EC_{50} is the concentration of agonist required to produce the half-maximal current. All data are presented as mean ± standard error of the mean (S.E.); n is the number of cells. Statistical significance was evaluated with paired Student's t-test (for parametric data) or Mann–Whitney rank sum test (for nonparametric data), $p < 0.05$ was considered statistically significant.

Acknowledgements

This work was supported by Fondo di Ricerca di Ateneo (University of Camerino). We thank Elena Sokolova for preliminary experiments on biological assay. The financial support of Telethon Foundation – Italy (Grant no. GGP10082) and of Cariplo Foundation to A. N. is gratefully acknowledged.

Appendix A. Supporting information

Supporting information related to this article can be found at http://dx.doi.org/10.1016/j.ejmech.2013.04.037.

References

[1] G. Burnstock, Purinergic mechanosensory transduction and visceral pain, Mol. Pain 5 (2009) 69.
[2] G. Burnstock, Purinergic signalling and disorders of the central nervous system, Nat. Rev. Drug Discov. 7 (2008) 575–590.
[3] T. Nakatsuka, J.G. Gu, P2X purinoceptors and sensory transmission, Pflügers Arch. 452 (2006) 598–607.
[4] C.C. Chen, A.N. Akopian, L. Sivilotti, D. Colquhoun, G. Burnstock, J.N. Wood, A P2X purinoceptor expressed by a subset of sensory neurons, Nature 377 (1995) 428–431.
[5] C. Lewis, S. Neidhart, C. Holy, R.A. North, G. Buell, A. Surprenant, Coexpression of P2X2 and P2X3 receptor subunits can account for ATP-gated currents in sensory neurons, Nature 377 (1995) 432–435.
[6] E.J. Bradbury, G. Burnstock, S.B. McMahon, The expression of P2X3 purinoreceptors in sensory neurons: effects of axotomy and glial-derived neurotrophic factor, Mol. Cell. Neurosci. 12 (1998) 256–268.
[7] B.A. Chizh, P. Illes, P2X receptors and nociception, Pharmacol. Rev. 53 (2001) 553–568.
[8] V. Souslova, P. Cesare, Y. Ding, A.N. Akopian, L. Stanfa, R. Suzuki, K. Carpenter, A. Dickenson, S. Boyce, R. Hill, D. Nebenuis-Oosthuizen, A.J. Smith, E.J. Kidd, J.N. Wood, Warm-coding deficits and aberrant inflammatory pain in mice lacking P2X3 receptors, Nature 407 (2000) 1015–1017.
[9] D.A. Cockayne, S.G. Hamilton, Q.M. Zhu, P.M. Dunn, Y. Zhong, S. Novakovic, A.B. Malmberg, G. Cain, A. Berson, L. Kassotakis, L. Hedley, W.G. Lachnit, G. Burnstock, S.B. McMahon, A.P. Ford, Urinary bladder hyporeflexia and reduced pain-related behaviour in P2X3-deficient mice, Nature 407 (2000) 1011–1015.
[10] X. Bian, J. Ren, M. DeVries, B. Schnegelsberg, D.A. Cockayne, A.P. Ford, J.J. Galligan, Peristalsis is impaired in the small intestine of mice lacking the P2X3 subunit, J. Physiol. 551 (2003) 309–322.
[11] M.F. Jarvis, Contributions of P2X3 homomeric and heteromeric channels to acute and chronic pain, Expert Opin. Ther. Targets 7 (2003) 513–522.
[12] K.J. Lynch, E. Touma, W. Niforatos, K.L. Kage, E.C. Burgard, T. van Biesen, E.A. Kowaluk, M.F. Jarvis, Molecular and functional characterization of human P2X(2) receptors, Mol. Pharmacol. 56 (1999) 1171–1181.
[13] B.R. Bianchi, K.J. Lynch, E. Touma, W. Niforatos, E.C. Burgard, K.M. Alexander, H.S. Park, H. Yu, R. Metzger, E. Kowaluk, M.F. Jarvis, T. van Biesen, Pharmacological characterization of recombinant human and rat P2X receptor subtypes, Eur. J. Pharmacol. 376 (1999) 127–138.
[14] M.F. Jarvis, B.S. Khakh, ATP-gated P2X cation-channels, Neuropharmacology 56 (2009) 208–215.
[15] J.D. Brederson, M.F. Jarvis, Homomeric and heteromeric P2X3 receptors in peripheral sensory neurons, Curr. Opin. Investig. Drugs 9 (2008) 716–725.
[16] K. Wirkner, B. Sperlagh, P. Illes, P2X(3) receptor involvement in pain states, Mol. Neurobiol. 36 (2007) 165–183.
[17] E.C. Burgard, W. Niforatos, T. van Biesen, K.J. Lynch, K.L. Kage, E. Touma, E.A. Kowaluk, M.F. Jarvis, Competitive antagonism of recombinant P2X(2/3) receptors by 2′,3′-*O*-(2,4,6-trinitrophenyl) adenosine 5′-triphosphate (TNP-ATP), Mol. Pharmacol. 58 (2000) 1502–1510.
[18] M.F. Jarvis, E.C. Burgard, S. McGaraughty, P. Honore, K. Lynch, T.J. Brennan, A. Subieta, T. Van Biesen, J. Cartmell, B. Bianchi, W. Niforatos, K. Kage, H. Yu, J. Mikusa, C.T. Wismer, C.Z. Zhu, K. Chu, C.H. Lee, A.O. Stewart, J. Polakowski, B.F. Cox, E. Kowaluk, M. Williams, J. Sullivan, C. Faltynek, A-317491, a novel potent and selective non-nucleotide antagonist of P2X3 and P2X2/3 receptors, reduces chronic inflammatory and neuropathic pain in the rat, Proc. Natl. Acad. Sci. U. S. A. 99 (2002) 17179–17184.
[19] C.E. Muller, Emerging structures and ligands for P2X(3) and P2X(4) receptors-towards novel treatments of neuropathic pain, Purinergic Signal. 6 (2010) 145–148.
[20] D. Carter, M.P. Dillon, R.C. Hawley, C.J.J. Lin, D.W. Parish, C.A. Broka, A. Jahangir, Diaminopyrimidines as P2X3 and P2X2/3 Antagonists, WO 2005/095359 A1, 2005.
[21] A.P. Ford, J.R. Gever, P.A. Nunn, Y. Zhong, J.S. Cefalu, M.P. Dillon, D.A. Cockayne, Purinoceptors as therapeutic targets for lower urinary tract dysfunction, Br. J. Pharmacol. 147 (Suppl. 2) (2006) S132–S143.
[22] R. Volpini, R.C. Mishra, D.D. Kachare, D. Dal Ben, C. Lambertucci, I. Antonini, S. Vittori, G. Marucci, E. Sokolova, A. Nistri, G. Cristalli, Adenine-based acyclic nucleotides as novel $P2X_3$ receptor ligands, J. Med. Chem. 52 (2009) 4596–4603.
[23] S. Calimsiz, M.G. Organ, Negishi cross-coupling of secondary alkylzinc halides with aryl/heteroaryl halides using Pd-PEPPSI-IPent, Chem. Commun. (Camb.) 47 (2011) 5181–5183.
[24] C. Lambertucci, I. Antonini, M. Buccioni, D. Dal Ben, D.D. Kachare, R. Volpini, K.N. Klotz, G. Cristalli, 8-Bromo-9-alkyl adenine derivatives as tools for developing new adenosine A_{2A} and A_{2B} receptors ligands, Bioorg. Med. Chem. 17 (2009) 2812–2822.
[25] G. Langli, L.-L. Gundersen, F. Rise, Regiochemistry in Stille couplings of 2,6-dihalopurines, Tetrahedron 52 (1996) 5625–5638.
[26] E. Fabbretti, E. Sokolova, L. Masten, M. D'Arco, A. Fabbro, A. Nistri, R. Giniatullin, Identification of negative residues in the P2X3 ATP receptor ectodomain as structural determinants for desensitization and the Ca^{2+}-sensing modulatory sites, J. Biol. Chem. 279 (2004) 53109–53115.
[27] D.A. Brown, D.I. Yule, Protein kinase C regulation of P2X3 receptors is unlikely to involve direct receptor phosphorylation, Biochim. Biophys. Acta 1773 (2007) 166–175.
[28] E. Sokolova, A. Skorinkin, E. Fabbretti, L. Masten, A. Nistri, R. Giniatullin, Agonist-dependence of recovery from desensitization of P2X(3) receptors provides a novel and sensitive approach for their rapid up or downregulation, Br. J. Pharmacol. 141 (2004) 1048–1058.
[29] E. Sokolova, A. Skorinkin, I. Moiseev, A. Agrachev, A. Nistri, R. Giniatullin, Experimental and modeling studies of desensitization of P2X3 receptors, Mol. Pharmacol. 70 (2006) 373–382.
[30] Molecular Operating Environment, C.C.G., Inc., 1255 University St., Suite 1600, Montreal, Quebec, Canada H3B 3X3.
[31] J.J. Stewart, MOPAC: a semiempirical molecular orbital program, J. Comput. Aided Mol. Des. 4 (1990) 1–105.
[32] M. Sundukova, S. Vilotti, R. Abbate, E. Fabbretti, A. Nistri, Functional differences between ATP-gated human and rat P2X3 receptors are caused by critical residues of the intracellular C-terminal domain, J. Neurochem. 122 (2012) 557–567.
[33] M. Simonetti, A. Fabbro, M. D'Arco, M. Zweyer, A. Nistri, R. Giniatullin, E. Fabbretti, Comparison of P2X and TRPV1 receptors in ganglia or primary culture of trigeminal neurons and their modulation by NGF or serotonin, Mol. Pain 2 (2006) 11.